*Microbiology* (2013), **159**, 12–22 DOI 10.1099/mic.0.062059-0

# High-resolution detection of DNA binding sites of the global transcriptional regulator GlxR in *Corynebacterium glutamicum*

Britta Jungwirth,[1] Claudia Sala,[2] Thomas A. Kohl,[1]† Swapna Uplekar,[2] Jan Baumbach,[3] Stewart T. Cole,[2] Alfred Pühler[1] and Andreas Tauch[1]

Correspondence
Andreas Tauch
tauch@cebitec.uni-bielefeld.de

[1]Institut für Genomforschung und Systembiologie, Centrum für Biotechnologie, Universität Bielefeld, Bielefeld, Germany

[2]Global Health Institute, Ecole Polytechnique Fédérale de Lausanne, Lausanne, Switzerland

[3]Computational Systems Biology, Max-Planck-Institut für Informatik, Saarbrücken, Germany

The transcriptional regulator GlxR has been characterized as a global hub within the gene-regulatory network of *Corynebacterium glutamicum*. Chromatin immunoprecipitation with a specific anti-GlxR antibody and subsequent high-throughput sequencing (ChIP-seq) was applied to *C. glutamicum* to get new *in vivo* insights into the gene composition of the GlxR regulon. In a comparative approach, *C. glutamicum* cells were grown with either glucose or acetate as the sole carbon source prior to immunoprecipitation. High-throughput sequencing resulted in 69 million reads and 2.6 Gb of genomic information. After mapping of these data on the genome sequence of *C. glutamicum*, 107 enriched DNA fragments were detected from cells grown with glucose as carbon source. GlxR binding sites were identified in the sequence of 79 enriched DNA fragments, of which 21 sites were not previously reported. Electrophoretic mobility shift assays with 40-mer oligomers covering the GlxR binding sites were performed for validation of the *in vivo* results. The detection of new binding sites confirmed the role of GlxR as a regulator of carbon source metabolism and energy conversion, but additionally revealed binding of GlxR in front of the 6C non-coding RNA gene and to non-canonical DNA binding sites within protein-coding regions. The present study underlines the dynamics within the GlxR regulon by identifying *in vivo* targets during growth on glucose and contributes to the expansion of knowledge of this important transcriptional regulator.

Received 10 July 2012
Revised 23 October 2012
Accepted 24 October 2012

## INTRODUCTION

In the age of massive sequencing of bacterial genomes, transcriptional regulatory networks (TRNs) are interesting to study in order to understand how the regulation of mRNA synthesis contributes to the dynamic expression of biological functions. These networks are composed of transcriptional regulatory proteins, their target genes and the regulatory interactions exerted (Babu *et al.*, 2004). Transcriptional regulatory proteins play a key role in the control of gene expression in prokaryotic cells, as they integrate different signals from the environment or the cellular metabolism to adapt the expression levels for an adequate response to changing conditions (Pollack & Iyer, 2002).

Various approaches exist to elucidate the structure and function of a prokaryotic TRN (Babu *et al.*, 2009). For *in vivo* investigations, DNA microarray experiments are used to compare distinct strains of a bacterial species or different growth conditions, thereby identifying regulated targets and transcriptional regulators involved (Dharmadi & Gonzalez, 2004; Rodionov, 2007). More recently, chromatin immunoprecipitation (ChIP) with specific antibodies against RNA polymerase or bacterial transcriptional regulators has been successfully applied (Laub *et al.*, 2002). The combination of ChIP with the detection of enriched DNA fragments on a DNA microarray (ChIP-chip) led to the global identification of binding regions for nucleoid-associated and transcriptional regulatory proteins in bacteria (Grainger & Busby, 2008; Wade *et al.*, 2007). Using high-throughput sequencing technologies, it is now possible to investigate the binding sites

†Present address: Molekulare Mycobakteriologie, Forschungszentrum Borstel, 23845 Borstel, Germany.

Abbreviations: ChIP, chromatin immunoprecipitation, ChIP-seq, ChIP with sequencing; COG, Clusters of Orthologous Groups; CRP, cAMP receptor protein; EMSA, electrophoretic mobility shift assay; IP, immunoprecipitation; PWM, position weight matrix; TRN, transcriptional regulatory network.

Three supplementary tables are available with the online version of this paper.

of DNA-interacting proteins by sequencing the immunoprecipitated fragments (ChIP-seq) (Park, 2009). The major advantage of ChIP-seq, when compared with ChIP-chip, is the higher resolution of binding site detection. Recently, this method was used for the first time in *Escherichia coli* to study the genome-wide distribution of the nucleoid-associated proteins Fis and H-NS (Kahramanoglou *et al.*, 2011). There are few further ChIP-seq studies in prokaryotes so far, reporting on binding of transcriptional regulators and a sigma factor of *Mycobacterium tuberculosis*, *Pseudomonas syringae* and *Vibrio cholerae* (Blasco *et al.*, 2012; Butcher *et al.*, 2011; Davies *et al.*, 2011; Markel *et al.*, 2011; Smollett *et al.*, 2012).

We applied ChIP-seq to the industrially relevant actinobacterium *Corynebacterium glutamicum* to characterize the regulon of the global transcriptional regulator GlxR. The Crp–Fnr family regulator GlxR is composed of an amino-terminal cAMP-binding domain and a carboxy-terminal DNA recognition helix–turn–helix motif, and interacts with its binding sites with the consensus sequence 5′-TGTGANNTANNTCACA-3′ in a cAMP-dependent manner (Han *et al.*, 2007; Jungwirth *et al.*, 2008; Kohl & Tauch, 2009; Kohl *et al.*, 2008). Many bacteria use cAMP as a second messenger in diverse signalling pathways (Botsford & Harman, 1992; Gomelsky, 2011; Rickemberg, 1974). In *C. glutamicum*, intracellular cAMP levels change depending on the metabolized carbon source. It has been shown that the amount of cAMP in *C. glutamicum* cells increases during growth on glucose and decreases during growth on acetate (Kim *et al.*, 2004).

The role of GlxR as an important hub in the TRN of *C. glutamicum* has been analysed by electrophoretic mobility shift assay (EMSA) *in vitro* or in artificial *in vivo* systems, such as promoter probe assays (reviewed by Schröder & Tauch, 2010). As a result, a large number of DNA binding sites have been identified. The reference database CoryneRegNet currently lists 151 GlxR-regulated genes (as of September 2012), including the autoregulation of GlxR (Baumbach *et al.*, 2009; Pauling *et al.*, 2012). A total of 215 potential GlxR binding sites were predicted bioinformatically based on current experimental data (Kohl & Tauch, 2009). Recently, a ChIP-chip experiment confirmed the global role of GlxR in transcriptional regulation, detecting 209 potential target regions genome-wide (Toyoda *et al.*, 2011). Among these, 84 regions contain previously described GlxR binding sites, and, based on motif discovery, 94 new binding motifs were identified. About one quarter (53/209) of the detected binding regions are presumably situated in coding regions or in intergenic regions between convergently organized genes (Toyoda *et al.*, 2011).

In the current study, we used ChIP-seq for the detection of DNA binding sites *in vivo*, and thereby confirmed that GlxR acts as a global transcriptional regulator in response to changing growth conditions, i.e. when comparing growth of *C. glutamicum* on glucose with that on acetate. Our data underline the role of GlxR as a regulator of alternative carbon source metabolism during growth on glucose and its implication in the control of many important cell functions, such as central metabolism, cell cycle control, cell wall turnover and stress responses.

## METHODS

**Bacterial cultivation.** *C. glutamicum* ATCC 13032 cells were grown under aerobic conditions at 30 °C in minimal medium CGXII (Keilhauer *et al.*, 1993) containing 30 mg protocatechuic acid $l^{-1}$ and 420 µg thiamine $l^{-1}$. The carbon source (40 g glucose $l^{-1}$) was replaced by 5 g acetate $l^{-1}$ where appropriate. *E. coli* JM109 cells containing plasmid pETCRP (Letek *et al.*, 2006) were grown under aerobic conditions at 37 °C in Luria–Bertani (LB) medium (Sambrook *et al.*, 1989) with 50 µg kanamycin $ml^{-1}$. Growth was monitored by measuring the $OD_{600}$ using a spectrophotometer (Eppendorf).

**Protein purification and antibody production.** Recombinant GlxR protein was expressed in *E. coli* JM109 cells carrying plasmid pETCRP and purified as described elsewhere (Letek *et al.*, 2006). The protein was washed and concentrated using Amicon Ultra-4 10K Centrifugal Filter units (Millipore). This preparation was used for commercial polyclonal antibody production in rabbits and for affinity purification of the anti-GlxR antiserum produced (Eurogentec).

**ChIP-seq.** The ChIP-seq protocol was based on previous experiments with *M. tuberculosis* (Sala *et al.*, 2009), and was modified for use on *C. glutamicum* cells. Exponentially growing *C. glutamicum* glucose and acetate cultures were treated with 1 % formaldehyde (final concentration). After 10 min of incubation at 30 °C with gentle shaking, glycine was added to a final concentration of 125 mM. Cells were harvested by centrifugation, washed twice with ice-cold PBS (pH 7.4) and stored at −20 °C. Pellets were resuspended to a final concentration of $5 \times 10^9$ cells $ml^{-1}$ in PBS with protease inhibitors (Mini Complete, Roche), and cell disruption was achieved using a RiboLyser (Precellys, Peqlab). Cell debris were removed by centrifugation and DNA in the supernatant was sheared to an average size of 200–500 bp by sonication in a water bath (Bioruptor, Diagenode). An input sample of 10 µl was taken and stored at −20 °C until RNase treatment. For immunoprecipitation (IP), 1 % Triton X-100, 0.1 % SDS and 0.1 % sodium deoxycholate (final concentrations) were added, and the samples were incubated overnight at 4 °C on a rotating wheel with 5 µg custom rabbit polyclonal anti-GlxR antibody $ml^{-1}$ (Eurogentec). Protein–DNA complexes were immunoprecipitated with 50 µl Dynabeads Protein G (Invitrogen) for 4 h at 4 °C. The magnetic beads were washed twice with IP buffer, once with IP buffer plus 500 mM NaCl, once with buffer III (10 mM Tris/HCl, pH 8, 250 mM LiCl, 1 mM EDTA, 0.5 % Nonidet-P40, 0.5 % sodium deoxycholate) and once with Tris-EDTA buffer (pH 7.5). For elution, beads were resuspended in 100 µl elution buffer (50 mM Tris/HCl, pH 7.5, 10 mM EDTA, 1 % SDS) and incubated at 65 °C for 30 min. IP and input samples were diluted with one volume of water and treated with RNase A. Proteinase K was added, and cross-linking was reversed by incubation at 50 °C for 2 h and 65 °C for 8 h. DNA was extracted with phenol/chloroform/isoamyl alcohol (25 : 24 : 1), precipitated and resuspended in water. DNA solutions were concentrated in a SpeedVac concentrator. Sequencing libraries with an average fragment size of 250 bp were prepared according to the Illumina ChIP-seq protocol and sequenced in a 38 bp single read run on an Illumina Genome Analyser IIx sequencing machine.

**Read mapping and data visualization.** Quality filtered reads were mapped to the *C. glutamicum* ATCC 13032 genome sequence (Kalinowski *et al.*, 2003) with SARUMAN (Blom *et al.*, 2011), allowing

for up to two errors per read (insertion, deletion and/or mismatch). Mapped sequence data were visualized using VAMP (Hackl *et al.*, 2011).

**Peak detection.** The in-house tool CISA (Chromatin Immunoprecipitation Sequence Analyzer) was used for peak detection. As a first step in the algorithm, for each sample the number of reads that mapped to a specific genomic position was counted for both strands separately. The absolute difference in read counts between a sample and the background and the enrichment factors (quotient of signal and background) were derived for each base position. Next, the absolute difference in the read counts curve was smoothed by performing a convolution with a Gaussian filter with a variance of 40 bp.

Local maxima with a threshold of at least 40 counts above background were identified from these smoothed signals on both strands. These maxima served as seed positions in the algorithm from which possible bi-modal enrichment patterns were identified afterwards. Therefore, for each peak on the forward or reverse strand, corresponding peaks on the other strand within a window of 60–155 bp downstream or upstream were identified, constrained to exhibit approximately equal height and enrichment factors. Both the forward/reverse and reverse/forward peak pairs were then intersected and reported as enriched DNA fragments.

Additional filtering was performed by comparing the positions of the maxima on the differential expressed signal maps with the positions of maxima on the original smoothed signal for each strand, discarding bi-modal patterns with deviations larger than 16 bp.

Two CISA runs were performed with the glucose IP sample using the input sample and the acetate IP sample as background, respectively. Only enriched fragments detected in both runs within a window of 20 bp were taken into account. A total of 14 peaks were removed manually because of their localization within *rrn* operons or the $tRNA^{Glu}$ and $tRNA^{Asp}$ genes. These regions show a high variation in read counts independently of IP due to the fact that their sequences are not unique in the genome.

The sequences of the detected enriched DNA fragments were extracted, taking the genomic positions of the two peaks on each strand as starting points and adding 60 bp on each side of the enriched DNA fragment to cover the fragment entirely.

**Motif analysis and genome-wide search for GlxR binding sites.** For *de novo* motif discovery within the significantly enriched DNA fragments, their genomic sequences were submitted to MEME (Bailey & Elkan, 1994). Parameters were set to search for zero or one palindromic motif of 16 bp width per sequence. A genome-wide search for GlxR binding sites was performed using the PoSSuMsearch algorithm (Beckstette *et al.*, 2006), as described previously (Kohl *et al.*, 2008), but without restriction to intergenic regions. The position weight matrix (PWM) model of the binding motif was built based on all DNA binding sites, for which *in vitro* binding of GlxR using 40 bp oligomers has been reported (Jungwirth *et al.*, 2008; Kohl & Tauch, 2009; Kohl *et al.*, 2008).

Based on the manually curated annotation of the *C. glutamicum* ATCC 13032 genome sequence (Kalinowski *et al.*, 2003) and the distribution of 452 (as of September 2012) regulator binding sites in *C. glutamicum* (Pauling *et al.*, 2012), upstream regions were defined for all coding sequences (CDSs) ranging from +20 to −600 bp relative to the translation start.

**Functional analysis of GlxR targets.** All genes for which GlxR binding was detected within the upstream or the coding region were considered to be target genes. They were classified according to their Clusters of Orthologous Groups (COG) categories. The distribution was compared with the COG distribution of all *C. glutamicum* genes. To test for statistical significance, two-sided *P* values were calculated using a Fisher's exact test as defined in Agresti (1992). The significance level was set to $P \leqslant 0.05$.

**DNA band shift assays.** EMSAs were carried out as established and validated previously (Jungwirth *et al.*, 2008; Kohl & Tauch, 2009; Kohl *et al.*, 2008), with the exception that 0.05 pmol labelled double-stranded DNA oligonucleotides were used. Oligomers were designed with the predicted GlxR binding motif in the centre and 12 bp of flanking genomic sequence on both sides. The oligonucleotide sequences for the binding sites with the genomic positions 804 771–804 786 and 2 305 775–2 305 790 were modified at the 3′ or 5′ ends of the flanking genomic regions to avoid secondary structure formation, as described previously (Kohl *et al.*, 2008).

## RESULTS

### IP of GlxR–DNA complexes and high-throughput sequencing

A specific anti-GlxR antibody was used in ChIP-seq experiments with the objective of gaining more detailed insights into the GlxR regulon. We investigated the influence of varying cAMP levels on GlxR binding in *C. glutamicum*, since the homologous Crp protein from *E. coli* has been reported to lose its DNA binding capacity under low-cAMP conditions (Grainger *et al.*, 2005). In *C. glutamicum*, intracellular cAMP levels are increased during growth on glucose and decrease during growth on acetate (Kim *et al.*, 2004); thus, these growth conditions were selected for ChIP-seq experiments. Comparison of protein extracts from glucose- and acetate-metabolizing cells in Western blots revealed similar amounts of GlxR protein (data not shown). ChIP samples were prepared from exponentially growing cultures metabolizing each of the two carbon sources, and DNA fragments were sequenced. Additionally, an input DNA sample was sequenced from glucose-metabolizing cells before IP. Each sample was sequenced on one lane of a 38 bp single-read run. Of the 22.7–23.8 million reads (862–902 Mb) sequenced, 22.0–22.8 million reads were uniquely mapped to the *C. glutamicum* ATCC 13032 genome sequence (Table 1). The mapped reads provided the basis for the detection of enriched DNA fragments and candidate GlxR binding sites.

### Detection of enriched DNA fragments

The characteristics of an enriched DNA fragment are exemplified in Fig. 1 for the promoter region of the acetaldehyde dehydrogenase gene *ald* containing a known GlxR binding site. The distinctive structure of a pair of (local) maxima of read counts or peaks is observed in the profile of the glucose IP sample, but not in those of the acetate IP or the input samples. The representations of two profiles in one diagram together with a third curve showing the calculated absolute difference between them (Fig. 1b) clearly demonstrates the enrichment in the glucose IP sample.

**Table 1.** Sequencing and mapping data for ChIP-seq with GlxR of *C. glutamicum*

| Sample | Sequencing data | | | Mapping data | |
|---|---|---|---|---|---|
| | Cluster (PF*) | Sequenced kilobases | Sequence reads | Mapped reads | Unmapped reads |
| ChIP-seq glucose | 77.8 ± 3.9 % | 902 506 | 23 750 157 | 22 845 356 | 904 801 |
| ChIP-seq acetate | 80.6 ± 4.2 % | 862 373 | 22 694 026 | 22 041 173 | 652 853 |
| Input control | 80.7 ± 4.3 % | 862 509 | 22 697 605 | 22 188 776 | 508 829 |

*PF, Passed filter.

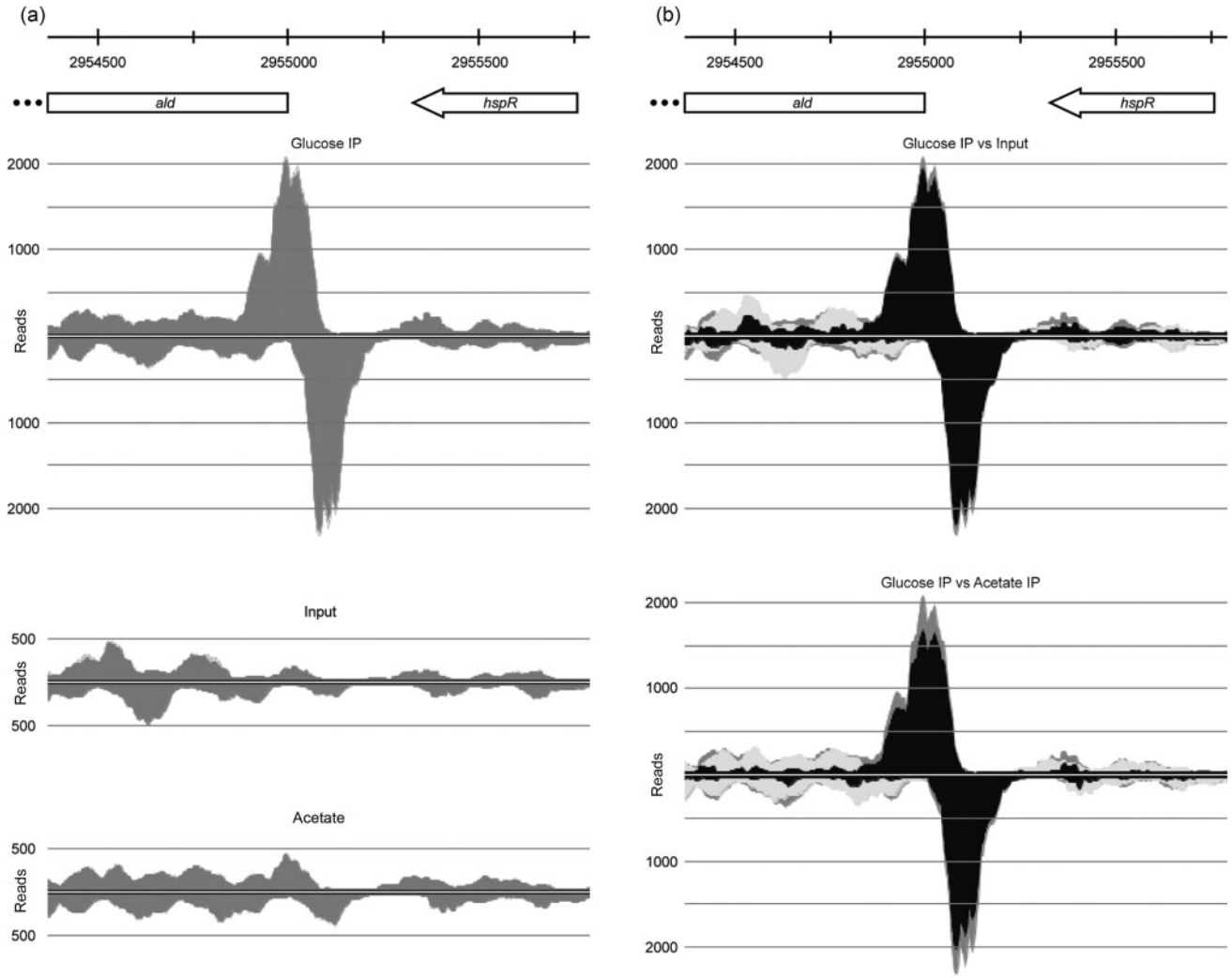


**Fig. 1.** Visualization of the sequencing results for the *ald* promoter region. The numbers of reads per basepair were counted for each of the three samples and are represented as profiles (a). The forward strand is shown on the upper scale and the reverse strand on the lower scale of each diagram. On the right-hand side, sequencing results for two samples are shown in one diagram as well as the absolute difference between them (b). The results from the glucose ChIP sample are represented as a dark-grey curve, the results from the second sample in light grey, and the absolute difference between the two in black. The curves are superposed with dark grey in the background, light grey in the middle and black in the foreground.

Inspection of the profiles at the genomic positions of previously known binding sites (Pauling *et al.*, 2012; Toyoda *et al.*, 2011) was performed in order to identify which sites had been enriched by IP with anti-GlxR antibody. The characteristic two-peak structure was present in the glucose IP sample for a subset of these sites. GlxR binding was identified for 32 DNA motifs that had shown interaction in EMSAs previously (Pauling *et al.*, 2012) and for 57 loci detected by ChIP-chip (Toyoda *et al.*, 2011). No or significantly less enrichment was observed in the acetate IP sample at GlxR binding sites. The data from the acetate IP sample were therefore used as a second background control for the automated peak detection with CISA, in addition to the input sample.

With CISA a total of 239 DNA fragments (see Table S1 available with the online version of this paper) were detected, which were enriched in the glucose IP sample over the input and the acetate IP sample. Enrichment factors were calculated as the quotient of read numbers in the glucose IP and the input sample, revealing a broad range of enrichment from 1.1- to 113.3-fold. Further analyses were focused on the 107 DNA fragments that were at least twofold enriched (Table S2). Out of the 107 DNA fragments, two were also enriched in the acetate IP sample over the input. They were localized in the *ald* promoter region (Fig. 1), which was 15.6-fold enriched in the glucose IP sample and 2.7-fold in the acetate IP sample, and in the intergenic region between the *pta–ack* operon and the *fpr1* gene. This region, containing a predicted binding site (Kohl & Tauch, 2009), was 3.4-fold enriched in the acetate IP sample.

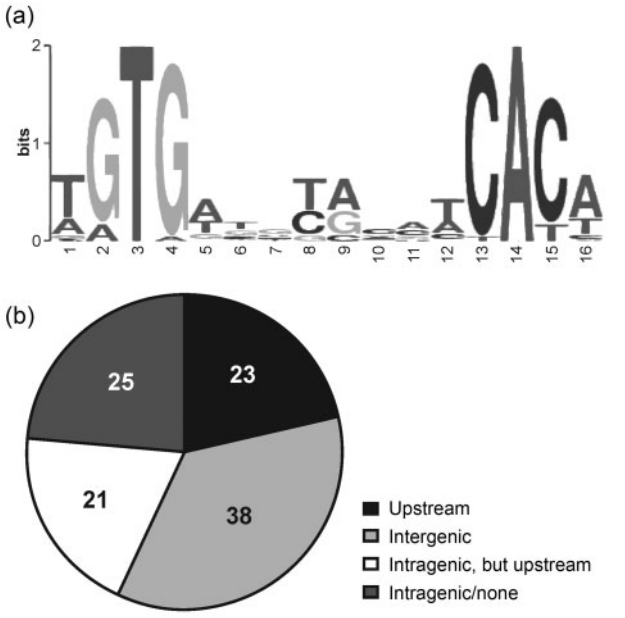


**Fig. 2.** (a) Weblogo of the motif detected with MEME (Bailey & Elkan, 1994) within the sequences of the 107 identified GlxR binding regions. (b) Distribution of the genomic localizations of the binding sites with regard to the closest situated genes. Binding within a region ranging from −600 bp to +20 bp relative to a translation start site was considered to be upstream of a transcription unit. Correspondingly, intergenic binding sites are situated in the shared upstream region of two divergently transcribed genes. For binding inside a coding sequence, we distinguished between purely intragenic positions (intragenic/none) and intragenic positions upstream of another divergent or convergent transcription unit (intragenic, but upstream).

## *De novo* motif search within enriched DNA fragments

The sequences of the 107 DNA fragments were submitted to the motif-based sequence analysis tool MEME (Bailey & Elkan, 1994) to detect conserved DNA motifs. The best common motif identified by MEME is shown in Fig. 2(a). The 16 bp palindromic sequence was found in 20 instances (18.7 % of cases) with an E-value of $3.6 \times 10^3$ (Table S3). This motif is very similar to the previously published consensus sequence TGTGANNTANNTCACA of GlxR binding sites that resulted from *in vitro* analyses (Kohl *et al.*, 2008). The *de novo* identification of the conserved GlxR motif within the sequences of the enriched DNA fragments validated the experimental approach. Nevertheless, the 20 detected motifs probably represent only a subset of all GlxR binding sites. The reason is that the search algorithm of MEME has been optimized for the detection of high conservation of a motif and not for the identification of all instances of a motif (Bailey & Elkan, 1994).

## GlxR motif prediction and comparison of *in vivo*, *in silico* and *in vitro* data

A PWM-based genome-wide search for GlxR binding sites was performed in order to validate the ChIP-seq data by a second *in silico* approach. This search procedure is advantageous for the detection of more instances of a given motif in the case of degenerate binding sites. In addition, it allows for the comparison of the ChIP-seq data with previous studies (Kohl & Tauch, 2009; Kohl *et al.*, 2008). Subsequently, the 107 enriched DNA fragments were classified according to the occurrence of validated GlxR binding sites from prior EMSA studies or putative motifs predicted by PoSSuMsearch in their sequences (Table S2). Binding sites reported previously to interact with GlxR in EMSAs were located within 32 DNA fragments, including the described autoregulatory binding site (Jungwirth *et al.*, 2008) in the *glxR* promoter region. Furthermore, 47 fragments contained at least one GlxR binding site predicted by PoSSuMsearch. About one quarter of all DNA fragments (28 out of 107) could not be associated with any DNA motif resembling the GlxR consensus binding site.

Additionally, the fragments were grouped into four categories in relation to the genomic position of the included motifs with regard to closely situated genes (Fig. 2b). For fragments without a motif, the genomic position

of the central 16 bp of the fragment was taken into account. The example of the *ald* gene (Fig. 1) illustrates GlxR binding upstream of a single transcription unit. Additional binding situations found within the dataset were: (i) intergenic binding upstream of two divergently orientated transcription units; (ii) intragenic binding inside a coding region; and (iii) intragenic binding upstream of a neighbouring gene. Examples of these genomic contexts of GlxR–DNA interaction are shown in Fig. 3. A special case is represented in Fig. 3(b), where protein binding in the intergenic region of the protein-coding gene *cg0360* and the small RNA 6C is shown.

Due to the experimental design, all binding sites validated by EMSA in previous studies were located in either upstream or intergenic regions (Table S2, upper part). Interestingly, 59.6 % of the GlxR motifs detected with PoSSuMsearch (28 out of 47) shared these genomic environments (Table S2, middle part). Furthermore, our study validates GlxR binding inside coding regions, which had been suggested by the recent ChIP-chip analysis (Toyoda *et al.*, 2011). With 19 out of 47 PoSSuMsearch-detected motifs and the majority of the fragments without a binding motif (27 out of 28) falling into this category, intragenic binding represented 43 % of the total of 107 GlxR–DNA interaction sites.

### EMSAs and functional analysis of the GlxR regulon

To further validate the ChIP-seq results *in vitro*, EMSAs were designed taking into consideration all possible genomic contexts of GlxR binding in relation to neighbouring genes. Two sets of predicted binding sites were chosen for validation by EMSA: eight motifs with an E-value from PoSSuMsearch smaller than 400 and eight motifs with a higher E-value (Table S2). Gel retardation was observed for all oligomers containing a low-E-value motif, demonstrating the interaction of GlxR with these motifs *in vitro* (Fig. 4a). In contrast, only 50 % of the oligomers containing a motif with a higher E-value showed interaction by EMSA (Fig. 4b). In all cases, GlxR binding was cAMP-dependent and no binding occurred without the cofactor.

The newly identified and validated motifs extend the knowledge of GlxR targets. Intragenic binding of GlxR protein was confirmed *in vitro* for the first time, to our knowledge, within the gene-coding sequences of *cg0875* and *cg0968*. The position of the motif in *cg0968* strongly suggests the presence of a promoter for the divergently transcribed gene *cg0967*, which could be under the control of GlxR. In contrast, there was no evidence from the genomic sequence of a promoter region situated close to the binding site inside the sequence of the *cg0875* gene. Additionally, binding was confirmed in the intergenic region of *cg0565* (*gabR*) and *gabT*, thereby involving GlxR in the control of the recently described $\gamma$-aminobutyric acid (GABA) metabolism (Zhao *et al.*, 2012) of *C. glutamicum*. Among the other validated targets, there were genes from carbohydrate metabolism (*iolR*, *iolC–cg0198–iolA–B–D–E–G–H* operon, *msiK2*, *prpD2–B2–C2* operon), transporter genes (*cg2610*, *cg1305*), a molecular chaperone gene (*hscA*) and a superfamily II DNA/RNA helicase gene (*cg1307*).

For a global view of the regulon composition during growth on glucose, all target genes identified by ChIP-seq were classified according to their COG category (data not shown). The resulting distribution was compared with the COG distribution of all annotated *C. glutamicum* genes. It is noteworthy that the percentages of GlxR targets were significantly (with a $P$ value $\leqslant 0.05$) elevated in the following five COG categories as compared with the genome: 'energy production and conversion' (C), 'carbohydrate transport and metabolism' (G), 'amino acid transport and metabolism' (E), 'inorganic ion transport and metabolism' (P), and 'secondary metabolites biosynthesis, transport and catabolism' (Q).

## DISCUSSION

In the present study, ChIP-seq was, for the first time to our knowledge, applied to *C. glutamicum*. The method has rarely been used for bacteria until now, although it has been routinely exploited in eukaryotic cells for several years. To our knowledge, seven ChIP-seq studies have been published on bacterial transcription factor, sigma factor and nucleoid-associated protein binding sites (Blasco *et al.*, 2012; Butcher *et al.*, 2011; Davies *et al.*, 2011; Jutras *et al.*, 2012; Kahramanoglou *et al.*, 2011; Markel *et al.*, 2011; Smollett *et al.*, 2012), and one dataset was used in a bioinformatics approach (Lun *et al.*, 2009). While epitope-tagged proteins were used in most of the above-mentioned studies, here, the Crp-family protein GlxR was immunoprecipitated with a specific antibody from cells growing on glucose or acetate as the sole carbon source. Sequencing of the ChIP samples in conjunction with automated peak finding led to the detection of 107 DNA fragments that were more than twofold enriched by IP from glucose-metabolizing *C. glutamicum* cells.

Recently, the importance of improving peak detection tools for ChIP-seq datasets has been underlined (Håndstad *et al.*, 2011; Rye *et al.*, 2011; Wilbanks & Facciotti, 2010). In our study, the method for peak detection relies on the characteristic features of a peak, such as the appearance of one read count maximum on the leading followed by a second maximum on the lagging strand. By using two background controls, the present study responds to another suggestion for amelioration (Rye *et al.*, 2011). Furthermore, we evaluated the ChIP-seq results using a *de novo* and a PWM-based motif discovery approach. This approach facilitated the comparison with existing data and led to the identification and *in vitro* validation of new binding sites. It might also be useful for the estimation of false positives detected by ChIP-seq, as the presence of a DNA motif resembling the GlxR consensus within an

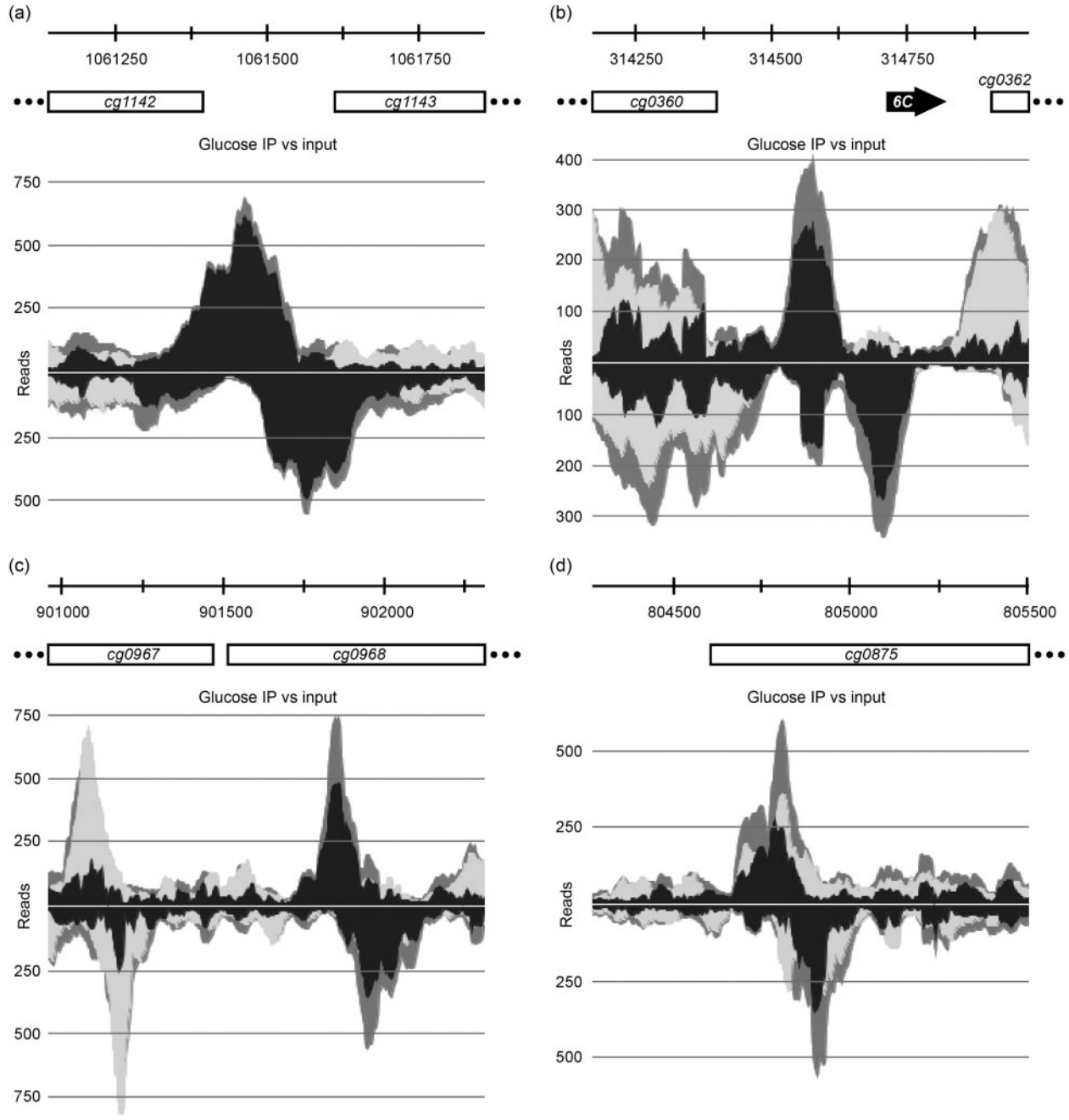


**Fig. 3.** Visualization of sequencing results for four enriched DNA fragments. Representation of (a) the intergenic region between *cg1142* and *cg1143*, (b) the intergenic region between the protein-coding gene *cg0360* and the small RNA 6C, (c) the intragenic binding within *cg0968* upstream of *cg0967*, and (d) the intragenic binding within *cg0875*. The peaks shown in (a) and (b) contain GlxR motifs located upstream of either of the two divergently transcribed genes, and the protein could be implicated in the regulation of both transcription units. The peaks in (c) and (d) are situated inside the coding sequence.

enriched fragment provides additional evidence for a true binding site. However, the *in vivo* situation can differ from *in silico* predictions and *in vitro* conditions. For detailed analysis of a specific binding site, further *in vivo* studies are needed, going far beyond the global picture given by ChIP-seq.

In accordance with the fact that GlxR is known to interact with DNA in a cAMP-dependent manner (Han *et al.*, 2007; Jungwirth *et al.*, 2008; Kim *et al.*, 2004; Kohl & Tauch, 2009; Kohl *et al.*, 2008), we observed significantly less or no DNA enrichment in acetate-metabolizing cells where the cAMP level was decreased. Similarly, a significant drop in

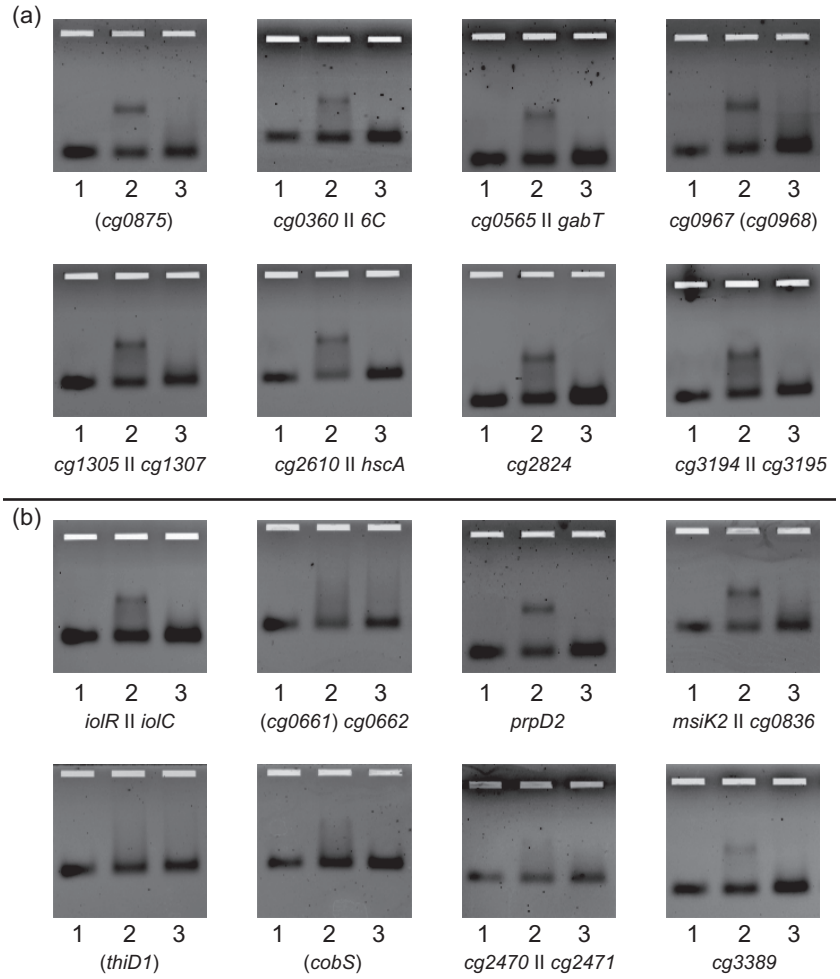


**Fig. 4.** EMSAs with purified GlxR protein and 40 bp oligonucleotides containing motifs detected by the genome-wide PoSSuMsearch with an E-value (a) below and (b) above 400. Lanes: 1, control assays containing only 40-mers; 2, DNA band shift assays containing 40-mers, purified GlxR protein and cAMP; 3, control assays containing 40-mers and purified GlxR protein.

the number of binding regions and the enrichment factors was described in a recent ChIP-chip study with GlxR (Toyoda *et al.*, 2011) after deletion of the *cyaB* gene, encoding the only known adenylate cyclase of *C. glutamicum*. Nevertheless, cAMP is still detectable in the *cyaB* deletion strain (Cha *et al.*, 2010), and the decrease of GlxR binding was not as marked as in our study (Toyoda *et al.*, 2011). The present result is also in accordance with the situation in *E. coli*, where lowering the intracellular cAMP level has been reported to result in a loss of cAMP receptor protein (CRP) binding by ChIP-chip (Grainger *et al.*, 2005). As the effect observed in our study was very drastic, and only two out of 107 fragments were also enriched after IP from acetate-grown cells, there are probably additional factors involved besides the differences in cAMP levels. An explanation might be the overlap in the function of GlxR with other transcriptional regulators such as RamA and RamB in acetate-metabolizing cells (reviewed by Schröder & Tauch, 2010).

GlxR is also directly connected to several other transcriptional regulator genes. Using ChIP-seq, *iolR*, *whcA*, *cg0343*, *gabR*, *whcE*, *cg1143*, *fruR*, *vanR*, *genR*, *cg3388* and the two-component system *citAB* were identified as GlxR targets during growth on glucose. GlxR is therefore involved in hierarchical regulation, which enables the cell to dynamically control the expression of different metabolic subsystems. This confirms the role of the GlxR protein as a global hub within the TRN of *C. glutamicum*.

The ChIP-seq experiment revealed GlxR binding in the upstream regions of genes for alternative carbon source uptake and metabolism. Interestingly, genes involved in the carbohydrate and central metabolism and transport systems (COG categories C, G, E, P and Q) were significantly enriched among GlxR targets as compared with the genome. The regulator thus shows some characteristics observed for homologous Crp proteins from *E. coli* and other Gram-negative bacteria in relation to carbon catabolite repression (Kolb *et al.*, 1993), even though the regulation of carbon metabolism is markedly different in *C. glutamicum*. Many substrates are co-metabolized by this organism, and monophasic growth is observed with only a few exceptions. The mixtures glucose/glutamate, glucose/ethanol and acetate/ethanol induce diauxic growth with preferential utilization of glucose or acetate (Arndt & Eikmanns, 2007; Arndt *et al.*, 2008; Kotrbova-Kozak *et al.*, 2007; Krämer *et al.*, 1990; Kronemeyer *et al.*, 1995). Interestingly, the enrichment

factors for three DNA fragments from the upstream regions of the genes for the acetaldehyde dehydrogenase (*ald*), the alcohol dehydrogenase (*adhA*) and the phosphotransacetylase–acetate kinase (*pta–ack*) operon, all needed for ethanol degradation, were, at 15.6, 11.9 and 18.3, among the highest observed enrichment factors. Moreover, GlxR binding was even detected during growth on acetate in the upstream regions of *ald* and *pta–ack* (enrichment factors: 3.4 and 2.7). This could be a clue to explain diauxic growth by a particularly high affinity of GlxR for these sites, leading to (nearly) complete repression in the presence of glucose.

Compared with previous studies including ChIP-chip (Bussmann *et al.*, 2009; Jungwirth *et al.*, 2008; Kim *et al.*, 2004; Kohl & Tauch, 2009; Kohl *et al.*, 2008; Letek *et al.*, 2006; Nishimura *et al.*, 2011; Panhorst *et al.*, 2011; Park *et al.*, 2010; Toyoda *et al.*, 2011), a total of 21 new binding sites and 46 corresponding target genes, including genes in predicted operons (Pauling *et al.*, 2012), were identified with ChIP-seq. Under the chosen growth conditions, GlxR interacted with 40 % (31 out of 77) of all DNA motifs from previous EMSA studies with 40 bp oligomers (Jungwirth *et al.*, 2008; Kohl & Tauch, 2009; Kohl *et al.*, 2008), and with one motif validated by EMSA with PCR products (Toyoda *et al.*, 2011). Comparison with the recent ChIP-chip study on GlxR binding showed an overlap of 57 fragments identified in both studies. The higher resolution of the ChIP-seq study allowed for the validated identification of intragenic sites for the first time, as the existence of such sites was only suggested by the microarray results. The 28 fragments without a predicted binding motif can be found among the 50 sites exclusively identified by ChIP-seq, pointing out the necessity of combining different approaches and techniques to fully elucidate the GlxR regulon.

The ChIP-seq results provide evidence of a non-protein-coding gene controlled by GlxR. The binding site in the shared upstream region of the gene for the small RNA 6C and the divergently transcribed gene *cg0360* was validated by EMSA. With its suggested function in sporulation, dormancy or metabolically inactive cell states (Swiercz *et al.*, 2008), the small RNA fits the profile of a GlxR target well. Further experiments will show the relevance of GlxR binding for the regulation of the 6C RNA. An example of a Crp regulator controlling the expression of a small RNA, *cyaR*, can be found in *E. coli* (De Lay & Gottesman, 2009).

We also describe GlxR as a non-canonical regulator, binding in intragenic regions. Beyond the regulon identified so far, there might be new mechanisms of action and targets to be detected outside the search space of promoter regions. For *E. coli* CRP, a role in chromosome structuring has been discussed based on ChIP-chip results, which revealed the presence of a large number of binding sites with low affinity (Grainger *et al.*, 2005). Other ChIP-chip and ChIP-seq datasets from eukaryotic cells also suggest a role for genome-wide transcription factors binding beyond direct target regulation (MacQuarrie *et al.*, 2011). In addition, at least for some of the GlxR binding regions lacking an evident correlation with a promoter region, new genetic features might be discovered in the future, for example by high-resolution RNA sequencing.

## ACKNOWLEDGEMENTS

B. J. acknowledges the receipt of a grant from the Studienstiftung des Deutschen Volkes. This work was supported by SystemsX.ch and the Swiss National Science Foundation under grant number 31003A-125061.

## REFERENCES

**Agresti, A. (1992).** A survey of exact inference for contingency tables. *Stat Sci* **7**, 131–153.

**Arndt, A. & Eikmanns, B. J. (2007).** The alcohol dehydrogenase gene *adhA* in *Corynebacterium glutamicum* is subject to carbon catabolite repression. *J Bacteriol* **189**, 7408–7416.

**Arndt, A., Auchter, M., Ishige, T., Wendisch, V. F. & Eikmanns, B. J. (2008).** Ethanol catabolism in *Corynebacterium glutamicum*. *J Mol Microbiol Biotechnol* **15**, 222–233.

**Babu, M. M., Luscombe, N. M., Aravind, L., Gerstein, M. & Teichmann, S. A. (2004).** Structure and evolution of transcriptional regulatory networks. *Curr Opin Struct Biol* **14**, 283–291.

**Babu, M. M., Lang, B. & Aravind, L. (2009).** Methods to reconstruct and compare transcriptional regulatory networks. *Methods Mol Biol* **541**, 163–180.

**Bailey, T. L. & Elkan, C. (1994).** Fitting a mixture model by expectation maximization to discover motifs in biopolymers. *Proc Int Conf Intell Syst Mol Biol* **2**, 28–36.

**Baumbach, J., Wittkop, T., Kleindt, C. K. & Tauch, A. (2009).** Integrated analysis and reconstruction of microbial transcriptional gene regulatory networks using CoryneRegNet. *Nat Protoc* **4**, 992–1005.

**Beckstette, M., Homann, R., Giegerich, R. & Kurtz, S. (2006).** Fast index based algorithms and software for matching position specific scoring matrices. *BMC Bioinformatics* **7**, 389.

**Blasco, B., Chen, J. M., Hartkoorn, R., Sala, C., Uplekar, S., Rougemont, J., Pojer, F. & Cole, S. T. (2012).** Virulence regulator EspR of *Mycobacterium tuberculosis* is a nucleoid-associated protein. *PLoS Pathog* **8**, e1002621.

**Blom, J., Jakobi, T., Doppmeier, D., Jaenicke, S., Kalinowski, J., Stoye, J. & Goesmann, A. (2011).** Exact and complete short-read alignment to microbial genomes using Graphics Processing Unit programming. *Bioinformatics* **27**, 1351–1358.

**Botsford, J. L. & Harman, J. G. (1992).** Cyclic AMP in prokaryotes. *Microbiol Rev* **56**, 100–122.

**Bussmann, M., Emer, D., Hasenbein, S., Degraf, S., Eikmanns, B. J. & Bott, M. (2009).** Transcriptional control of the succinate dehydrogenase operon *sdhCAB* of *Corynebacterium glutamicum* by the cAMP-dependent regulator GlxR and the LuxR-type regulator RamA. *J Biotechnol* **143**, 173–182.

**Butcher, B. G., Bronstein, P. A., Myers, C. R., Stodghill, P. V., Bolton, J. J., Markel, E. J., Filiatrault, M. J., Swingle, B., Gaballa, A. & other authors (2011).** Characterization of the Fur regulon in *Pseudomonas syringae* pv. tomato DC3000. *J Bacteriol* **193**, 4598–4611.

**Cha, P. H., Park, S. Y., Moon, M. W., Subhadra, B., Oh, T. K., Kim, E., Kim, J. F. & Lee, J. K. (2010).** Characterization of an adenylate cyclase gene (*cyaB*) deletion mutant of *Corynebacterium glutamicum* ATCC 13032. *Appl Microbiol Biotechnol* **85**, 1061–1068.

**Davies, B. W., Bogard, R. W. & Mekalanos, J. J. (2011).** Mapping the regulon of *Vibrio cholerae* ferric uptake regulator expands its known network of gene regulation. *Proc Natl Acad Sci U S A* **108**, 12467–12472.

**De Lay, N. & Gottesman, S. (2009).** The Crp-activated small noncoding regulatory RNA CyaR (RyeE) links nutritional status to group behavior. *J Bacteriol* **191**, 461–476.

**Dharmadi, Y. & Gonzalez, R. (2004).** DNA microarrays: experimental issues, data analysis, and application to bacterial systems. *Biotechnol Prog* **20**, 1309–1324.

**Gomelsky, M. (2011).** cAMP, c-di-GMP, c-di-AMP and now cGMP: bacteria use them all! *Mol Microbiol* **79**, 562–565.

**Grainger, D. C. & Busby, S. J. (2008).** Methods for studying global patterns of DNA binding by bacterial transcription factors and RNA polymerase. *Biochem Soc Trans* **36**, 754–757.

**Grainger, D. C., Hurd, D., Harrison, M., Holdstock, J. & Busby, S. J. (2005).** Studies of the distribution of *Escherichia coli* cAMP-receptor protein and RNA polymerase along the *E. coli* chromosome. *Proc Natl Acad Sci U S A* **102**, 17693–17698.

**Hackl, M., Jakobi, T., Blom, J., Doppmeier, D., Brinkrolf, K., Szczepanowski, R., Bernhart, S. H., Höner Zu Siederdissen, C., Bort, J. A. & other authors (2011).** Next-generation sequencing of the Chinese hamster ovary microRNA transcriptome: identification, annotation and profiling of microRNAs as targets for cellular engineering. *J Biotechnol* **153**, 62–75.

**Han, S. O., Inui, M. & Yukawa, H. (2007).** Expression of *Corynebacterium glutamicum* glycolytic genes varies with carbon source and growth phase. *Microbiology* **153**, 2190–2202.

**Håndstad, T., Rye, M. B., Drabløs, F. & Sætrom, P. (2011).** A ChIP-Seq benchmark shows that sequence conservation mainly improves detection of strong transcription factor binding sites. *PLoS ONE* **6**, e18430.

**Jungwirth, B., Emer, D., Brune, I., Hansmeier, N., Pühler, A., Eikmanns, B. J. & Tauch, A. (2008).** Triple transcriptional control of the resuscitation promoting factor 2 (*rpf2*) gene of *Corynebacterium glutamicum* by the regulators of acetate metabolism RamA and RamB and the cAMP-dependent regulator GlxR. *FEMS Microbiol Lett* **281**, 190–197.

**Jutras, B. L., Bowman, A., Brissette, C. A., Adams, C. A., Verma, A., Chenail, A. M. & Stevenson, B. (2012).** EbfC (YbaB) is a new type of bacterial nucleoid-associated protein and a global regulator of gene expression in the Lyme disease spirochete. *J Bacteriol* **194**, 3395–3406.

**Kahramanoglou, C., Seshasayee, A. S., Prieto, A. I., Ibberson, D., Schmidt, S., Zimmermann, J., Benes, V., Fraser, G. M. & Luscombe, N. M. (2011).** Direct and indirect effects of H-NS and Fis on global gene expression control in *Escherichia coli*. *Nucleic Acids Res* **39**, 2073–2091.

**Kalinowski, J., Bathe, B., Bartels, D., Bischoff, N., Bott, M., Burkovski, A., Dusch, N., Eggeling, L., Eikmanns, B. J. & other authors (2003).** The complete *Corynebacterium glutamicum* ATCC 13032 genome sequence and its impact on the production of L-aspartate-derived amino acids and vitamins. *J Biotechnol* **104**, 5–25.

**Keilhauer, C., Eggeling, L. & Sahm, H. (1993).** Isoleucine synthesis in *Corynebacterium glutamicum*: molecular analysis of the *ilvB–ilvN–ilvC* operon. *J Bacteriol* **175**, 5595–5603.

**Kim, H. J., Kim, T. H., Kim, Y. & Lee, H. S. (2004).** Identification and characterization of *glxR*, a gene involved in regulation of glyoxylate bypass in *Corynebacterium glutamicum*. *J Bacteriol* **186**, 3453–3460.

**Kohl, T. A. & Tauch, A. (2009).** The GlxR regulon of the amino acid producer *Corynebacterium glutamicum*: detection of the corynebacterial core regulon and integration into the transcriptional regulatory network model. *J Biotechnol* **143**, 239–246.

**Kohl, T. A., Baumbach, J., Jungwirth, B., Pühler, A. & Tauch, A. (2008).** The GlxR regulon of the amino acid producer *Corynebacterium glutamicum*: *in silico* and *in vitro* detection of DNA binding sites of a global transcription regulator. *J Biotechnol* **135**, 340–350.

**Kolb, A., Busby, S., Buc, H., Garges, S. & Adhya, S. (1993).** Transcriptional regulation by cAMP and its receptor protein. *Annu Rev Biochem* **62**, 749–797.

**Kotrbova-Kozak, A., Kotrba, P., Inui, M., Sajdok, J. & Yukawa, H. (2007).** Transcriptionally regulated *adhA* gene encodes alcohol dehydrogenase required for ethanol and *n*-propanol utilization in *Corynebacterium glutamicum* R. *Appl Microbiol Biotechnol* **76**, 1347–1356.

**Krämer, R., Lambert, C., Hoischen, C. & Ebbighausen, H. (1990).** Uptake of glutamate in *Corynebacterium glutamicum*. 1. Kinetic properties and regulation by internal pH and potassium. *Eur J Biochem* **194**, 929–935.

**Kronemeyer, W., Peekhaus, N., Krämer, R., Sahm, H. & Eggeling, L. (1995).** Structure of the *gluABCD* cluster encoding the glutamate uptake system of *Corynebacterium glutamicum*. *J Bacteriol* **177**, 1152–1158.

**Laub, M. T., Chen, S. L., Shapiro, L. & McAdams, H. H. (2002).** Genes directly controlled by CtrA, a master regulator of the *Caulobacter* cell cycle. *Proc Natl Acad Sci U S A* **99**, 4632–4637.

**Letek, M., Valbuena, N., Ramos, A., Ordóñez, E., Gil, J. A. & Mateos, L. M. (2006).** Characterization and use of catabolite-repressed promoters from gluconate genes in *Corynebacterium glutamicum*. *J Bacteriol* **188**, 409–423.

**Lun, D. S., Sherrid, A., Weiner, B., Sherman, D. R. & Galagan, J. E. (2009).** A blind deconvolution approach to high-resolution mapping of transcription factor binding sites from ChIP-seq data. *Genome Biol* **10**, R142.

**MacQuarrie, K. L., Fong, A. P., Morse, R. H. & Tapscott, S. J. (2011).** Genome-wide transcription factor binding: beyond direct target regulation. *Trends Genet* **27**, 141–148.

**Markel, E., Maciak, C., Butcher, B. G., Myers, C. R., Stodghill, P., Bao, Z., Cartinhour, S. & Swingle, B. (2011).** An extracytoplasmic function sigma factor-mediated cell surface signaling system in *Pseudomonas syringae* pv. tomato DC3000 regulates gene expression in response to heterologous siderophores. *J Bacteriol* **193**, 5775–5783.

**Nishimura, T., Teramoto, H., Toyoda, K., Inui, M. & Yukawa, H. (2011).** Regulation of the nitrate reductase operon *narKGHJI* by the cAMP-dependent regulator GlxR in *Corynebacterium glutamicum*. *Microbiology* **157**, 21–28.

**Panhorst, M., Sorger-Herrmann, U. & Wendisch, V. F. (2011).** The *pstSCAB* operon for phosphate uptake is regulated by the global regulator GlxR in *Corynebacterium glutamicum*. *J Biotechnol* **154**, 149–155.

**Park, P. J. (2009).** ChIP-seq: advantages and challenges of a maturing technology. *Nat Rev Genet* **10**, 669–680.

**Park, S. Y., Moon, M. W., Subhadra, B. & Lee, J. K. (2010).** Functional characterization of the *glxR* deletion mutant of *Corynebacterium glutamicum* ATCC 13032: involvement of GlxR in acetate metabolism and carbon catabolite repression. *FEMS Microbiol Lett* **304**, 107–115.

**Pauling, J., Röttger, R., Tauch, A., Azevedo, V. & Baumbach, J. (2012).** CoryneRegNet 6.0 – updated database content, new analysis methods and novel features focusing on community demands. *Nucleic Acids Res* **40** (Database issue), D610–D614.

**Pollack, J. R. & Iyer, V. R. (2002).** Characterizing the physical genome. *Nat Genet* **32** (Suppl.), 515–521.

**Rickemberg, H. V. (1974).** Cyclic AMP in prokaryotes. *Annu Rev Microbiol* **28**, 353–369.

**Rodionov, D. A. (2007).** Comparative genomic reconstruction of transcriptional regulatory networks in bacteria. *Chem Rev* **107**, 3467–3497.

**Rye, M. B., Sætrom, P. & Drabløs, F. (2011).** A manually curated ChIP-seq benchmark demonstrates room for improvement in current peak-finder programs. *Nucleic Acids Res* **39**, e25.

**Sala, C., Haouz, A., Saul, F. A., Miras, I., Rosenkrands, I., Alzari, P. M. & Cole, S. T. (2009).** Genome-wide regulon and crystal structure of BlaI (Rv1846c) from *Mycobacterium tuberculosis*. *Mol Microbiol* **71**, 1102–1116.

**Sambrook, J., Fritsch, E. & Maniatis, T. (1989).** *Molecular Cloning: a Laboratory Manual*, 2nd edn. Cold Spring Harbor, NY: Cold Spring Harbor Laboratory.

**Schröder, J. & Tauch, A. (2010).** Transcriptional regulation of gene expression in *Corynebacterium glutamicum*: the role of global, master and local regulators in the modular and hierarchical gene regulatory network. *FEMS Microbiol Rev* **34**, 685–737.

**Smollett, K. L., Smith, K. M., Kahramanoglou, C., Arnvig, K. B., Buxton, R. S. & Davis, E. O. (2012).** Global analysis of the regulon of the transcriptional repressor LexA, a key component of SOS response in *Mycobacterium tuberculosis*. *J Biol Chem* **287**, 22004–22014.

**Swiercz, J. P., Hindra, Bobek, J., Haiser, H. J., Di Berardo, C., Tjaden, B. & Elliot, M. A. (2008).** Small non-coding RNAs in *Streptomyces coelicolor*. *Nucleic Acids Res* **36**, 7240–7251.

**Toyoda, K., Teramoto, H., Inui, M. & Yukawa, H. (2011).** Genome-wide identification of *in vivo* binding sites of GlxR, a cyclic AMP receptor protein-type regulator in *Corynebacterium glutamicum*. *J Bacteriol* **193**, 4123–4133.

**Wade, J. T., Struhl, K., Busby, S. J. & Grainger, D. C. (2007).** Genomic analysis of protein–DNA interactions in bacteria: insights into transcription and chromosome organization. *Mol Microbiol* **65**, 21–26.

**Wilbanks, E. G. & Facciotti, M. T. (2010).** Evaluation of algorithm performance in ChIP-seq peak detection. *PLoS ONE* **5**, e11471.

**Zhao, Z., Ding, J. Y., Ma, W. H., Zhou, N. Y. & Liu, S. J. (2012).** Identification and characterization of $\gamma$-aminobutyric acid uptake system GabPCg (NCgl0464) in *Corynebacterium glutamicum*. *Appl Environ Microbiol* **78**, 2596–2601.

Edited by: D. Grainger